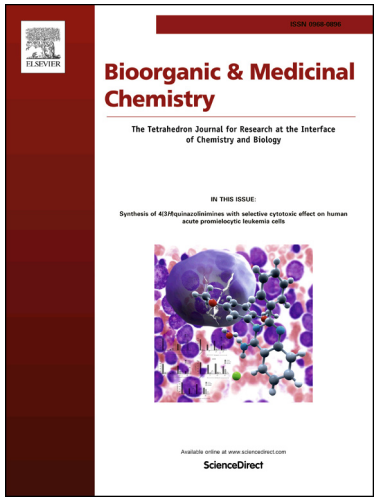


# Discovery of indolin-2-one derivatives as potent PAK4 inhibitors: Structure-activity relationship analysis, biological evaluation and molecular docking study

Jing Guo, Mingyue Zhu, Tianxiao Wu, Chenzhou Hao, Kai Wang, Zizheng Yan, Wanxu Huang, Jian Wang, Dongmei Zhao, Maosheng Cheng

PII: S0968-0896(17)30848-9
DOI: http://dx.doi.org/10.1016/j.bmc.2017.04.047
Reference: BMC 13719

To appear in: *Bioorganic & Medicinal Chemistry*

Received Date: 21 April 2017
Revised Date: 26 April 2017
Accepted Date: 28 April 2017

Please cite this article as: Guo, J., Zhu, M., Wu, T., Hao, C., Wang, K., Yan, Z., Huang, W., Wang, J., Zhao, D., Cheng, M., Discovery of indolin-2-one derivatives as potent PAK4 inhibitors: Structure-activity relationship analysis, biological evaluation and molecular docking study, *Bioorganic & Medicinal Chemistry* (2017), doi: http://dx.doi.org/10.1016/j.bmc.2017.04.047

# Discovery of indolin-2-one derivatives as potent PAK4 inhibitors: Structure-activity relationship analysis, biological evaluation and molecular docking study

Jing Guo[a], Mingyue Zhu[a], Tianxiao Wu[a], Chenzhou Hao[a], Kai Wang[a], Zizheng Yan[a], Wanxu Huang[a,b], Jian Wang[a], Dongmei Zhao[*,a], Maosheng Cheng[*, a]

[a] Key Laboratory of Structure-Based Drug Design & Discovery of Ministry of Education, Shenyang Pharmaceutical University, Shenyang 110016, China. E-mail: mscheng@263.net, dongmeiz-67@163.com; Fax: +86-24-23995043; Tel: +86-24-43520219

[b] School of Life Science and Bio-pharmaceutics, Shenyang Pharmaceutical University, Shenyang 110016, PR China

## Abstract

Utilizing a pharmacophore hybridization approach, a novel series of substituted indolin-2-one derivatives were designed, synthesized and evaluated for their *in vitro* biological activities against p21-activated kinase 4. Compounds **11b**, **12d** and **12g** exhibited the most potent inhibitory activity against PAK4 ($IC_{50}$ = 22 nM, 16 nM and 27 nM, respectively). Among them, compound **12g** showed the highest antiproliferative activity against A549 cells ($IC_{50}$ = 0.83 μM). Apoptosis analysis in A549 cells suggested that compound **12g** delayed cell cycle progression by arresting cells in the G2/M phase of the cell cycle, retarding cell growth. Further investigation demonstrated that compound **12g** strongly inhibited migration and invasion of A549 cells. Western blot analysis indicated that compound **12g** potently inhibited the PAK4/LIMK1/cofilin signalling pathways. Finally, the binding mode between compound **12g** with PAK4 was proposed by molecular docking. A preliminary ADME profile of the compound **12g** was also drawn on the basis of QikProp predictions.

**Keywords:** p21-activated kinase; PAK4 inhibitor; Indolin-2-one; Structure-activity relationship; Molecular docking

## 1. Introduction

The p21-activated kinases (PAKs), are a family of six serine/threonine kinases widely expressed across tissues that phosphorylate a number of proteins associated with functions as diverse as proliferation, apoptosis, and metastasis[1-4]. The six mammalian isoforms of PAKs are classified into two groups based on biochemical and structural features: group I, including PAK1, PAK2 and PAK3, and group II, including PAK4, PAK5 and PAK6[5]. PAK1 activity may contribute to tumourigenesis in some disease contexts[6, 7]. Importantly, it has recently been shown that acute cardiovascular toxicity result from the inhibition of PAK2, which may be enhanced by PAK1 inhibition, leading to doubts as to the validity of group I PAKs as drug targets[8]. PAK4 is the most extensively and profoundly studied member among the group II PAKs. It is not only highly overexpressed in several cancer cells but is also known to cause tumourigenesis[1]. Therefore, PAK4 is a promising target in the development of cancer therapeutics.

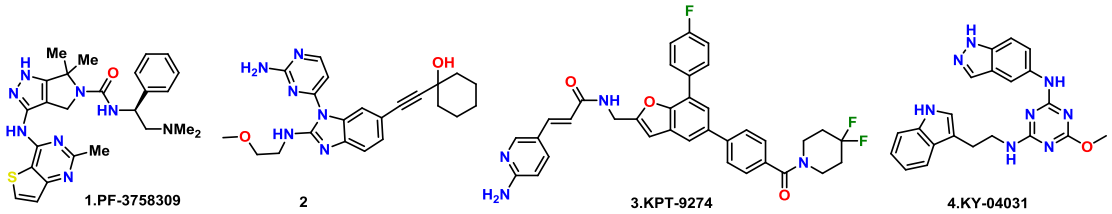

**Figure 1.** Structures of potent and selective PAK4 inhibitors.

A few potent and selective PAK4 inhibitors have been disclosed (**Figure 1**). For example, Compound **1** (PF-3758309) was progressed into phase I clinical trials in patients with advanced/metastatic solid tumours. Although designed to be a PAK4 inhibitor, the compound is, in fact, a pan-PAK inhibitor[9]. Unfortunately, PF-3758309 was prematurely discontinued in a single clinical trial due to undesirable pharmacokinetic characteristics[10]. Researchers from Genentech succeeded in identifying a highly potent and group II PAK-selective inhibitor series with exquisite kinome selectivity[11]. Compound **2** displayed PAK4 activity and > 870-fold selectivity over PAK1 ( PAK1 $K_i$ = 2.9 μM, PAK4 $K_i$ = 0.0033 μM )[11]. Recently, Karyopharm Therapeutics has identified a new class of dual PAK4/nicotinamide phosphoribosyltransferase (NAMPT) inhibitors that show anti-proliferative activity against several pancreatic cancer cell lines ($IC_{50}$ < 250 nM)[12, 13]. Compound **3** (KPT-9274) was progressed into phase I clinical trials in May 2016[14]. Compound **4** (KY-04031) was discovered using high-throughput screening. The unique molecular feature of KY-04031 can be exploited in designing new PAK4 inhibitors[15, 16].

Derivatives of the indolin-2-one scaffold are a prototypical class of protein kinase inhibitors[17-23]. Sunitinib and Nintedanib (**Figure 2**) are the representative drugs that emerged from indolin-2-one (2-oxindole) and are in clinical use for targeted anticancer therapies[10]. While it was reported that sunitinib was a weak inhibitor of the type II PAKs ($K_i$ is estimated in the range of 500 - 7000 nM for type II PAKs), it displayed selectivity for type II over type I PAK family members[24, 25]. The selectivity of indolin-2-ones against particular kinases is mediated by substituents on the indolin-2-one core. Particularly, the structural modifications at the C3- and C5-positions of the indolin-2-one ring have led to many derivatives possessing increased antitumour activity[26].

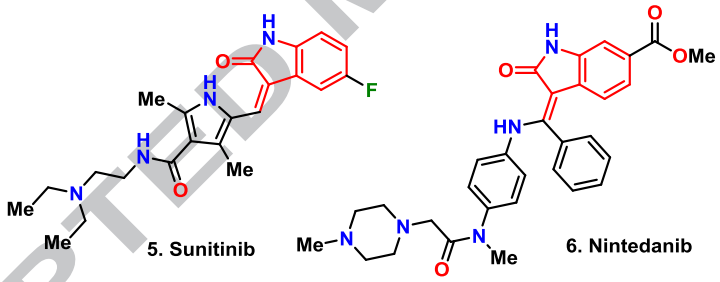


**Figure 2.** Representative examples of 3-alkenyl-indolin-2-one kinase inhibitors in clinical trials.

Guided by superposition of the crystal conformation of PF-3758309 (cyan) at the ATP-binding site of PAK4 with the predicted binding modes of Sunitinib (green) with the PAK4 (PDB code: 2x4z), we hypothesized that further extending at the C5-position of Sunitinib into the ribose pocket and P-loop would improve potency (**Figure 3**). In the development of novel PAK4 inhibitors, our design process incorporated indolin-2-one nucleus as the hinge binding group due to its planar geometrical conformation and possessing critical hydrogen bond donors and acceptors to interact with the amino acid residues of the kinases hinge region. Furthermore, Our efforts were focused on varying substituents at the 3, 5, and 6 positions of the indolin-2-one nucleus to capture additional interactions (**Figure 3**). The diethylaminoethyl amide tail group of Sunitinib that is exposed to solvent without specific contacts with protein was removed at present. On the basis of above strategy, we reported the synthesis, structure-activity relationship (SAR) study and *in vitro* biological evaluation of 24 novel 3-heterocyclic-5-amide substituted indolin-2-one derivatives as PAK4 inhibitors. The new compounds (**11a-q**, **12a-g**) were profiled against PAK4. Furthermore, we also explored the effects of selected compounds towards the cells proliferation, cells cycle progression, apoptosis, cells migration/invasion and possible mechanism of inducing migration/invasion on A549 cells.

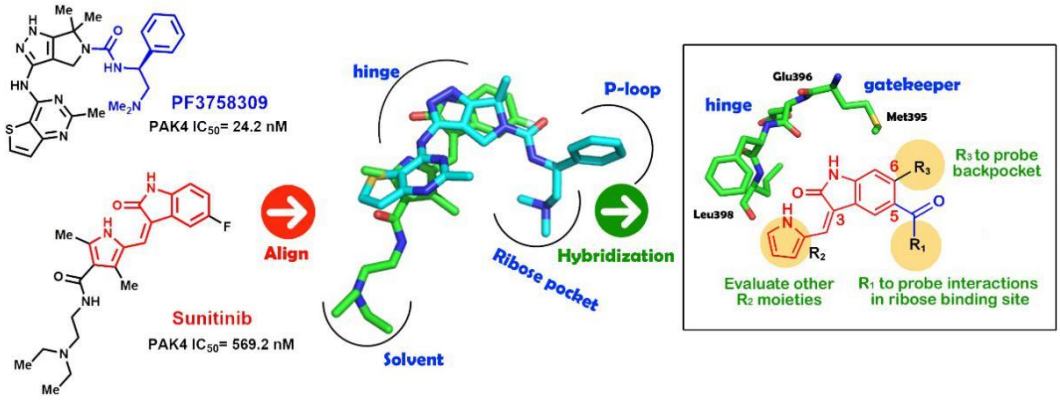


**Figure 3.** Rational design of the target compounds.

## 2. Results and discussion

### 2.1. Chemistry

The target compounds (**11a-q**, **12a-g**) were prepared following the procedure reported in **Scheme 1**. For the synthesis of 3-pyrrol indolin-2-one derivatives (**11a–n**), oxindole (**7**) was reacted with chloroacetyl chloride to yield compound **8**. Then, treatment of compound **8** with pyridine afforded an oxindole pyridinium salt, which was subsequently hydrolysed under basic conditions to yield intermediate **9**. Upon amidation with different amines ($R_1NH_2$) in the presence of 1-ethyl-3-(3-dimethylaminopropyl)-carbodiimide hydrochloride (EDC-HCl) and N-hydroxybenzotriazole (HOBt), intermediate **9** was converted to 5-carboxamides **10a-n**. Finally, the target compounds **11a-n** were obtained by condensation of 5-substituted indolin-2-one **10a-n** with pyrrole-2-carboxaldehyde in the presence of piperidine as the base catalyst. For the preparation of **11o-q**, commercially available 6-bromo indolin-2-one (**7d**) was converted to **11n** in four steps. Compound **11n**, which contains a reactive bromine at position 6, was further derivatized by Suzuki cross-coupling with a series of boronic acids esters or by cross-coupling with zinc cyanide catalysed by palladium to obtain compounds **11o-q**. Likewise, intermediate **10b** was converted to 3-substituted indolin-2-ones **12a-g** by Knoevenagel condensation, employing available aldehydes in the presence of piperidine as the base catalyst.

**Scheme 1**. Preparation of Compounds **11a-q**, **12a-g**.

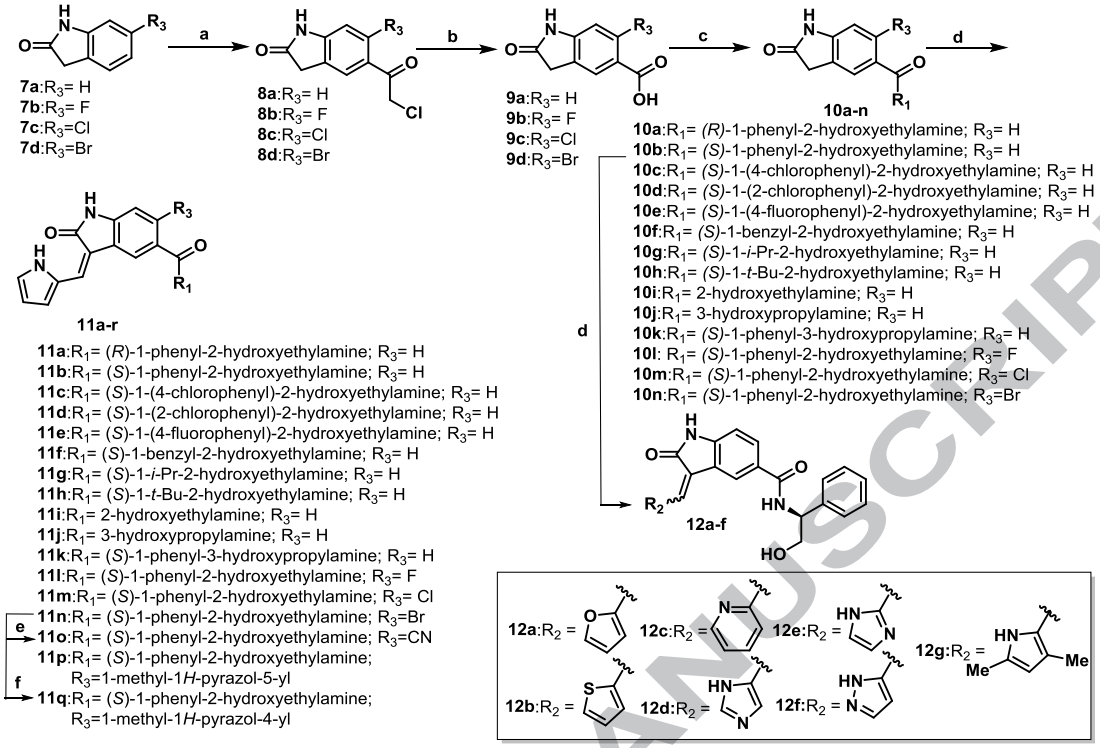


Reagents and conditions: (a) chloroacetyl chloride, anhydrous $AlCl_3$, 1,2-dichloroethane, r.t, 4.0 h. 80-92%. (b) i.pyridine, 90 °C, 3 h; ii. 2.5N NaOH (aq), 100 °C, 3.0 h, 85-97%. (c) $R_1$-$NH_2$, EDCI, HOBt, DIPEA, anhydrous DCM, r.t, 16 h, 63-88%. (d) appropriate aldehyde, piperidine, EtOH, sealed tube, 90 °C, 4.5 h, 59-90%. (e) $Zn(CN)_2$, $Pd(PPh_3)_4$, dry DMF, 85 °C, 46%. (f) $R_3$ boronic ester, $Pd(PPh_3)_4$, $K_2CO_3$, toluene/EtOH, reflux, 16 h, 58-69%.

## 2.2. Assignment of configuration of synthesized compounds

The 3-substituted indolin-2-ones may exist as either the *Z* or *E* isomer depending on the characteristics of the substituents at the C-3 position of the 3-substituted indolin-2-one (**Scheme 2**). Compounds containing a pyrrole substituent at the C-3 position of the 3-substituted indolin-2-ones existed exclusively as the Z isomer. A diagnostic feature is the intramolecular hydrogen bonding between the C-2 carbonyl oxygen atom of the indolin-2-one ring and the proton on the N-1′ of the pyrrole ring[27].

3-[(substituted furanyl)methylidenyl]indolin-2-ones (**12a**) appear to favour the E isomer form. This may be due to the electrostatic repulsion between the C-2 carbonyl oxygen atom of the indolin-2-one and the O-1′ of furan in the *Z* isomer. Indolin-2-ones having a 3-substituted thienyl group (**12b**) existed as *Z/E* mixtures although a sharp prevalence of *Z*-isomer has been observed (see supplementary data). Compound **12c**, which has a 3-substituted pyridine group, existed as the *E* isomer, probably due to the unfavourable interaction between the lone pair of the nitrogen of the pyridine ring and the carbonyl oxygen atom of the indolin-2-one ring in the *Z*-configured form. Indolin-2-ones that have a 3-substituted imidazole or pyrazole group (**12d**, **12e**, **12f**) existed as *Z/E* mixture (*Z* isomer is still the major form), probably due to imidazole or pyrazole tautomerization resulting in the loss of intramolecular hydrogen bonding (see supplementary data for details). (the vinyl hydrogen for the *E* isomer resonated downfield to the *Z* isomer by ~ 0.2-0.3 ppm due to deshielding effect of the carbonyl group of indolin-2-one moiety.)

**Scheme 2**. Assignment of Configuration of 3-Substituted Indolin-2-ones.

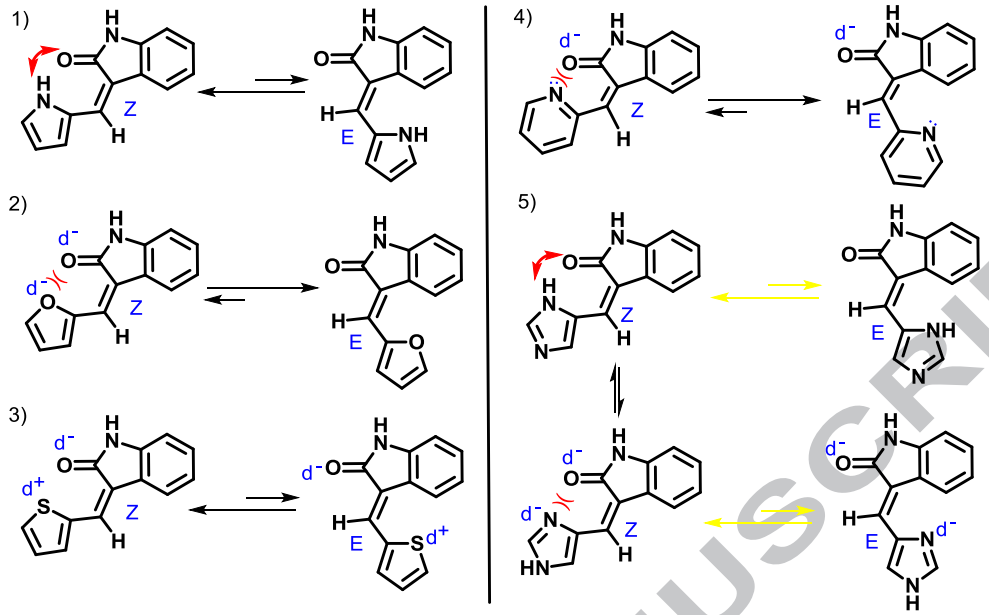


## 2.3. *In Vitro* Activity against PAK4 Kinase and SAR Analyses.

The *in vitro* inhibition of PAK4 kinase activity of the newly synthesized compounds was evaluated using an HTRF based kinase assay. One reported inhibitor of PAK4, compound **1**, was included to validate the screening conditions. Under the experimental conditions, compound **1** inhibited the activity of PAK4 with an $IC_{50}$ value of 24 nM (**Table 1**), which was similar to previously reported data[9].

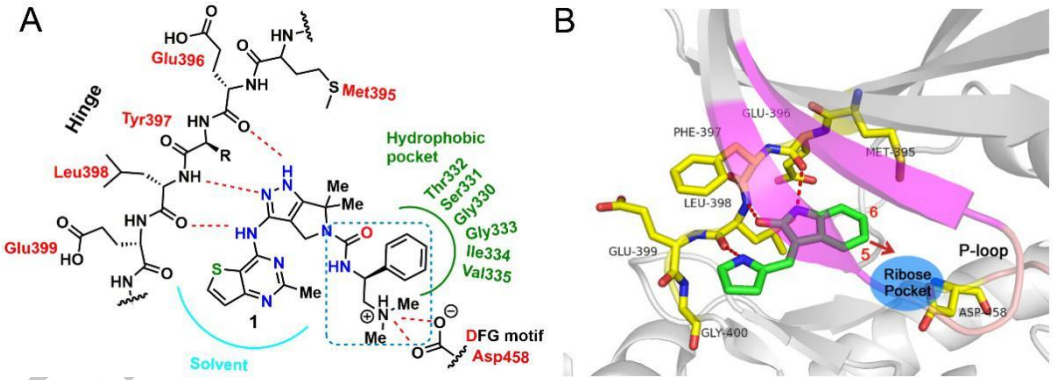


**Figure 4**. (A) PF-3758309 taken from its crystal structure with PAK4 (PDB: 2x4z). (B) 3-(pyrrol-2-yl)methylene-2-indolinone scaffold (green) modeled with PAK4. The red arrow highlights the vector off the 5-position of the 3-(pyrrol-2-yl)methylene-2-indolinone scaffold to grow toward the ribose pocket and P-loop.

At the outset of this study, the indolin-2-one scaffold as well as the pyrrole moiety were fixed, and structural variation was introduced by the synthesis of different amides groups (**Table 1**). In order to place a suitable fragment mimicking the N-2-(dimethylamino)-1-phenylethyl of compound **1** (**Figure 4**), phenylglycinol was to be grafted at the C5-positions of the indolin-2-one ring to develop compounds able to interact with the side chain carbonyl group of Asp458 of the DFG motif and the P-loop. Therefore, we merged the 3-(pyrrol-2-yl)methylene-2-indolinone scaffold with *D/L*-phenylglycinol, which provided analogues **11a** and **11b**. **11a** showed diminished enzymatic activity ($IC_{50}$ = 3376 nM), while **11b** had a beneficial effect ($IC_{50}$ = 22 nM). The *S*-enantiomer **11b** was 153-fold more potent than the *R*-enantiomer **11a**, emphasizing the importance of the *S*-enantiomer being a better fit with the phenyl group inserted into the glycine rich loop. Hence, further optimization work focused on *S*-enantiomer. Then, we investigated the substituent effects on the phenyl moiety of

phenylglycinol. Incorporation of a chlorine atom at the 4-position or 2-position of the phenyl ring provided **11c** and **11d**, respectively, both of which displayed measurable decreases in potency ($IC_{50}$ values of 391, 199 nM, respectively). Furthermore, introduction of a fluorine atom at the 4-position of the phenyl ring afforded **11e**, which was also not tolerated ($IC_{50}$ = 54 nM). Replacement of the phenyl group of **11b** with a larger benzyl or smaller *i*-propyl and *t*-butyl groups provided **11f**, **11g**, and **11h**, with dramatically decreased enzyme activity ($IC_{50}$ values of 304, 2355 and 634 nM, respectively). Removal of the phenyl ring afforded **11i**, which lost the most activity ($IC_{50}$ = 1255 nM). Compounds **11j** and **11k** which are homologues of **11i** and **11b** displayed either greater than 150-fold loss of potency or completely loss of potency ($IC_{50}$ values of 3145, 5005 nM, respectively). The potency loss of these analogues might be explained by the PAK4 P-loop pocket minor size and rigidity. Therefore, **11b** with an *L*-phenylglycinol substitution pattern was chosen as the compound for further optimization.

**Table 1**. Effect of $R_1$ Substituents on PAK4 biochemical $IC_{50}$ (nM).

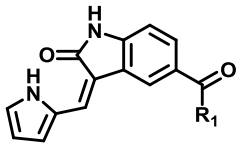

| Compd | $R_1$ | PAK4, $IC_{50}$ (nM)[c,d] | Compd | $R_1$ | PAK4, $IC_{50}$ (nM)[c,d] |
|---|---|---|---|---|---|
| **11a**[a] | 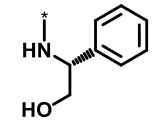 | 3376 | **11g** | 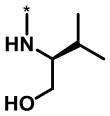 | 2355 |
| **11b**[b] | 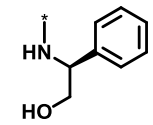 | 22 | **11h** | 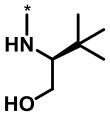 | 634 |
| **11c** | 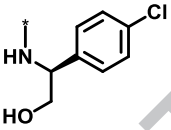 | 391 | **11i** | 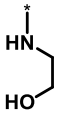 | 1255 |
| **11d** | 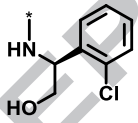 | 199 | **11j** | 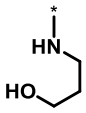 | 3145 |
| **11e** | 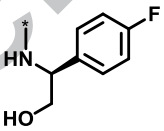 | 54 | **11k** | 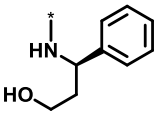 | 5005 |
| **11f** | 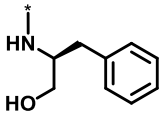 | 304 | **PF-3758309**[e] | - | 24 |

[a] *D*-phenylglycinol, *R*-enantiomer. [b] *L*-phenylglycinol, *S*-enantiomer. [c] $IC_{50}$ values are calculated based on the homogeneous time-resolved fluorescence (HTRF) assay. [d] Reported data are the mean values from two independent experiments. [e] Used as a positive control.

We next turned our attention to the pyrrole moiety by replacing it with other heterocyclics (**Table 2**). *In vitro* kinase assays with compounds **12a**, **12b**, and **12c** confirmed the importance of the pyrrole NH, which forms a hydrogen bond with the PAK4 hinge region. Seeking alternatives to the pyrrole provided compounds **12d**, **12e**, and **12f** respectively. Interestingly, when the imidazole nitrogen was moved to the 4'-position, the resulting compound **12d** was more potent than the 3'- or 5'-position analogues (**12e** and **12f**, respectively). These results implied that

the 4'-imidazole isomer interacted in a more favourable manner with the protein hinge residue. It's reported that the alkyl substituents on the 3'- or 5'-position of the pyrrole could destabilize interactions with a subset of off-target kinases[28]. Consistent with this idea, we prepared **12g**, which was nearly equipotent to **11b** in the enzymatic assay.

**Table 2**. Effect of $R_2$ Substituents on PAK4 biochemical $IC_{50}$ (nM).

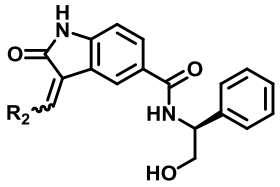

| Compd | $R_2$ | PAK4, $IC_{50}$ (nM)[a,b] | Compd | $R_2$ | PAK4, $IC_{50}$ (nM)[a,b] |
|---|---|---|---|---|---|
| **12a** |  | 802 | **12e** | 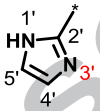 | 281 |
| **12b** |  | 1290 | **12f** | 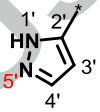 | 379 |
| **12c** |  | >10000 | **12g** | 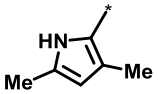 | 27 |
| **12d** | 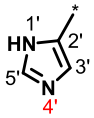 | 16 | **PF-3758309**[c] | - | 24 |

[a] $IC_{50}$ values are calculated based on the homogeneous time-resolved fluorescence (HTRF) assay. [b] Reported data are the mean values from two independent experiments. [c] Used as a positive control.

The vector of the C6 position on the oxindole is in the direction of a lipophilic pocket beyond the "gatekeeper" residue (Met-395 for PAK4). Access to this pocket affords enhancements in the activity and sometimes selectivity of inhibitors and was our next area of investigation (**Table 3**). As a general trend, introduction of substituents bearing hydrogen bond acceptors and their sizes was important for binding to the back pocket[29-31].

However, substitution at C6 with the small lipophilic F, Cl and Br substituents in compounds **11l**, **11m** and **11n**, respectively, was not tolerated. Increasing the size of the substituent even moderately (**11o**) produced a significant reduction in activity as well. Small-sized heterocycles with hydrogen bond acceptor capability such as pyrazole analogues (**11p-q**) either abolished or greatly reduced activity, presumably due to deleterious steric interactions with the gatekeeper residue Met-395, which prevented access to the lipophilic pocket.

**Table 3**. Effect of $R_3$ Substituents on PAK4 biochemical $IC_{50}$ (nM).

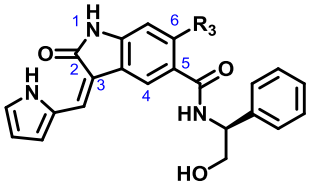

| Compd | $R_3$ | PAK4, $IC_{50}$ (nM)[a,b] | Compd | $R_3$ | PAK4, $IC_{50}$ (nM)[a,b] |
|---|---|---|---|---|---|
| **11l** | **F** | 718 | **11o** | **CN** | 1544 |

| | | | | | |
|---|---|---|---|---|---|
| **11m** | **Cl** | 1423 | **11p** |  | 1454 |
| **11n** | **Br** | 1201 | **11q** | 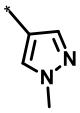 | 1987 |

[a] $IC_{50}$ values are calculated based on the homogeneous time-resolved fluorescence (HTRF) assay. [b] Reported data are the mean values from two independent experiments.

## 2.4. Antiviability Activities of Selected Compounds against Cancer Cell Lines.

The three compounds whose $IC_{50}$ values were lower than 30 nM were further evaluated for *in vitro* anticancer screening. Their $IC_{50}$ values against MCF-7 cell line and A549 cell line, in which PAK4 has been found to be overexpressed, were tested and listed in **Tables 4**. Meanwhile, the tumour cell line HT-1080, whose growth was not dependent on PAK4, was used to test the potential off-target effects of the potent PAK4 inhibitors. As shown in **Table 4**, the $IC_{50}$ values of these compounds against different tumour cells ranged between 0.83 and 10.80 μM except for compound **12d**, to which MCF-7 cells are not sensitive to and therefore do not experience decrease cell proliferation.

**Table 4**. Relative $IC_{50}$ (**μM**) values for selected compounds against A549, MCF-7 and HT-1080 cells lines.

| Compound | PAK4 | $IC_{50}$ (μM)[a] | | |
|---|---|---|---|---|
| | ($IC_{50}$, nM) | A549 | MCF-7 | HT-1080 |
| **11b** | 22 | 2.37 | 6.56 | 0.98 |
| **12d** | 16 | 3.70 | 10.80 | 7.90 |
| **12g** | 27 | 0.83 | 2.11 | 6.77 |

[a] $IC_{50}$: concentration of the compound (μM) producing 50% cell growth inhibition after 72 h of drug exposure, as determined by the CCK-8 assay.

## 2.5. Effects of Compound 12g on Cell Apoptosis and Cell Cycle Progression.

The ability of compound **12g** to induce tumour cell apoptosis was tested. The cells were harvested and stained with 7-aminoactinomycin D (7-AAD) and annexin-V, and the percentage of apoptotic cells was determined by flow cytometry analysis. As shown in **Figure 4A**, compound **12g** induced apoptosis in cells in a concentration-dependent manner. At a concentration of 5.0 μM, an apoptosis rate of 65.4% was observed after 72 h. We further examined the influence of compound **12g** on the cell cycle by using flow cytometry. When A549 cells were treated with **12g** at 1.0 μM or 5.0 μM, the number of cells in G2/M phase increased from 17.62% to 24.37% and 33.75%, whereas cells in G0/G1 phase decreased from 44.99% to 35.7% and 27.78%, respectively (**Figure 4B, C**). Taken together, these data demonstrated that compound **12g** could effectively lead to cell apoptosis and G2/M phase arrest in A549 cells.

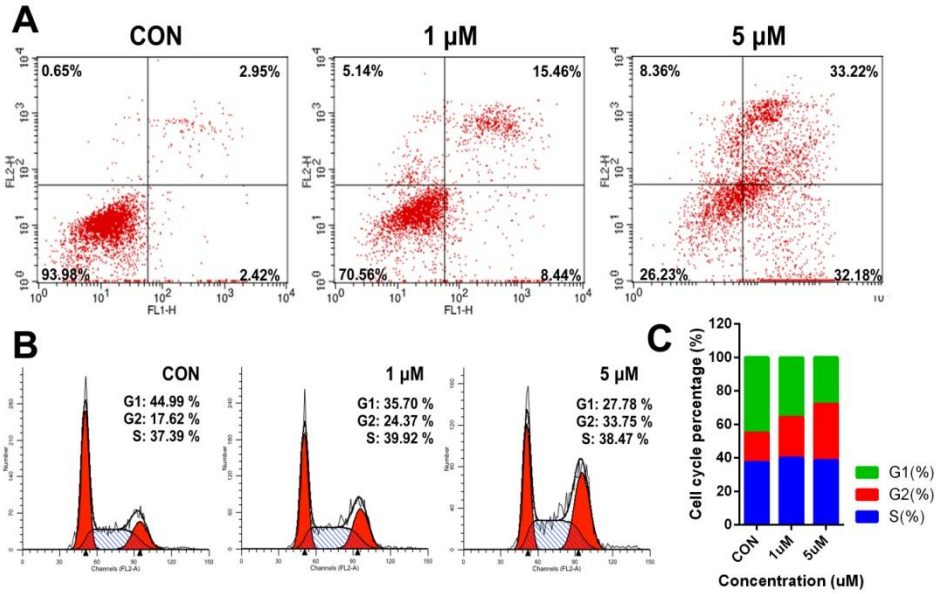


**Figure 4.** (A). Compound **12g** induced cell apoptosis. The cells were incubated with the indicated concentrations of **12g** for 72 h, and the cells were stained with 7-AAD and annexin-V, followed by flow cytometry analysis. (B). Compound **12g** induced G2/M cell cycle arrest of A549 cells. A549 cells were harvested after treatment with various concentrations of compound **12g** for 72 h. (C). Quantitative analysis of cell cycle.

## 2.6. Effects of Compound 12g on Tumor Cell Migration and Invasion

The effects of compound **12g** on tumour cell migration and invasion were assessed using transwell assays. As displayed in **Figure 5A**, after treatment of compound **12g** at a concentration of 5.0 μM for 72 h, the migration of A549 cells was significantly inhibited. The results from the transwell assays showed that 5.0 μM **12g** potently blocked the invasion ability of A549 cells. These results demonstrated that **12g** could efficiently exhibit antimetastatic potential against cancer cells.

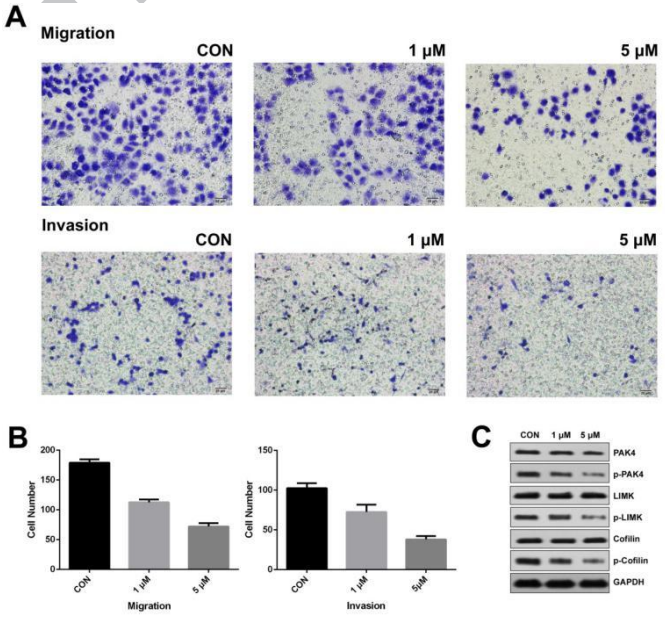


**Figure 5**. (A). Compound **12g** suppresses migration and invasion of A549 cells in transwell assays. The images were captured using phase contrast microscopy after 72 h of treatment. Scale bar, 20 μm. (B). Quantitative analysis of migration and invasion. (C). Compound **12g** inhibits phosphorylation of PAK4 and downstream signalling in A549 cells after 72 h treatments.

## 2.7. Inactivation of Key Signalling Proteins in A549 cells.

To further elucidate the mechanism of the inhibition of cancer cell migration and invasion, the expression of cellular signalling molecules was determined by Western blot analysis. Previous work showed that the PAK4/LIMK1/cofilin signalling pathway is correlated with cellular migration and invasion behaviour[32]. We therefore investigated the effects of compound **12g** on the PAK4/LIMK1/cofilin signalling pathway to validate its strong PAK4 kinase inhibition. As shown in **Figure 5C**, compound **12g** inhibited PAK4 phosphorylation in a dose-dependent manner. As expected, we observed inhibition of PAK4 downstream signalling protein LIMK1 and cofilin phosphorylation dose-dependently.

## 2.8. Binding mode analysis

To investigate potential binding modes, compound **12g** was docked into the ATP-binding site of PAK4 (PDB entry 2x4z) using Autodock 4.2. The predicted binding mode of **12g** to PAK4 is shown in **Figure 6**, in which the indolin-2-one scaffold forms two hydrogen bonds to the backbone carbonyl oxygen of Glu-396 and the NH of Leu-398 in the hinge region. Meanwhile, the carbonyl oxygen atom of the amide attached to the 5-position of indolin-2-one framework served as an H-bond acceptor for catalytic residue Lys-350, the conserved lysine in kinases that also forms a salt bridge with Glu-366 of the C-helix in the active conformation. The primary hydroxyl group interacted with the side chains of residue Asp-458 of the DFG motif. Beyond these H-bond interactions, the phenyl group of **12g** inserted into a small hydrophobic pocket under the P-loop and generated substantial hydrophobic contacts with neighbouring residues.

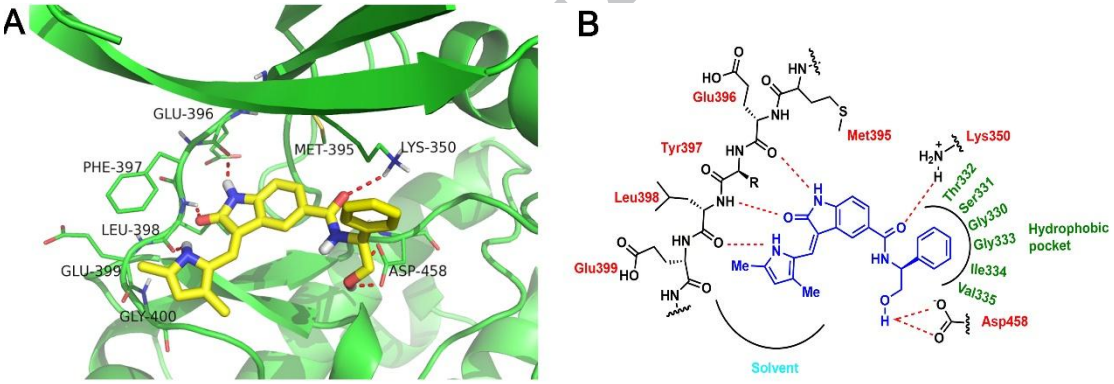


**Figure 6**. Molecular docking of **12g** in the ATP-binding site of PAK4. (A) Detailed interactions with the protein residues. Hydrogen bonds are rendered as red dotted lines. (B) 2D interaction diagram showing compound **12g** docking pose interactions with the key amino acids in the PAK4 active site.

## 2.9. ADME profiling of 12g

In recent years, there has been considerable discussion on the importance of optimizing the absorption, distribution, metabolism, and excretion (ADME) properties of drug candidates, in addition to their efficacy, to increase the rate of drug discovery successes and to advance high quality candidates to clinical studies. To further characterize the druglikeness of the most promising compounds **11b**, **12d** and **12g**, several physicochemical parameters were calculated, including lipophilicity (clogP), topological polar surface area (tPSA), molecular weight (MW), ligand efficiency (LE), ligandlipophilicity efficiency (LLE)[33], and ligand-efficiency-dependent lipophilicity (LELP)[34]. The clogP value was in all cases close to 3, which is in agreement with the general requirements for druglikeness and within the optimal range for orally administered drugs (clogP $\approx$ 3)[35, 36]. Additionally, the MW falls within the scope for optimal bioavailability (MW < 400 g $mol^{-1}$)[37]. Moreover, the estimated tPSA values were lower than 120. To evaluate the lipophilicity and structural contributions to *in vitro* potency[35], LE, LLE, and LELP were calculated using the $pIC_{50}$ from *in vitro* PAK4 inhibition data. All compounds displayed acceptable LE, LLE, and LELP values within the preferred range for good hits and leads[34].

**Table 5**. Druglikeness of Compounds **11b**, **12d** and **12g**.[a]

| *Entry* | *MW (g/mol)* | *pIC50*[b] | *clogP*[c] | *tPSA (Å)*[d] | *LE*[e] | *LLE*[f] | *LELP*[g] |
|---|---|---|---|---|---|---|---|
| **11b** | 373.410 | 7.66 | 2.84 | 106.88 | 0.38 | 4.82 | 7.42 |
| **12d** | 374.398 | 7.79 | 1.93 | 121.74 | 0.39 | 5.86 | 4.95 |
| **12g** | 401.464 | 7.56 | 3.47 | 106.41 | 0.35 | 4.09 | 9.83 |

[a]Properties determined using QikProp, version 4.3, Schrödinger, LLC, New York, NY, 2015. [b]$pIC_{50}$ = -log[$IC_{50}$ (PAK4, mol/L)]. [c]Partition coefficient. [d]Topological polar surface area. [e]LE = -1.4(log[$IC_{50}$ (PAK4, mol/L)/number of heavy atoms]). [f]LLE = $pIC_{50}$ - clogP. [g]LELP = clogP/LE.

## 3. Conclusion

In this study, a novel series of PAK4 inhibitors bearing a 3,5,6-trisubstituted indolin-2-one scaffold were designed and synthesized. Structure-activity relationships of these compounds were discussed based on enzymatic activities. Several compounds showed high potencies in biochemical functional assays. The three most active compounds were selected to be evaluated for their anticancer activity against A549, MCF-7 and HT1080 cells, of which **12g** exhibited the most potent anti-A549 cell activity. Further in-depth studies were carried out on **12g** for its biological assessment. The results showed that **12g** could effectively block the migration and invasion of A549 cells and lead to apoptosis and G2/M phase arrest. Western blot indicated that compound **12g** potently inhibited PAK4/LIMK1/cofilin signaling pathways. Finally, the binding mode between compound **12g** with PAK4 was proposed by molecular docking. Drug-likeness predictions indicate the capability of drug development of compound **12g**. Further investigations on these advanced leads are ongoing and will be reported in due course.

## 4. Experimental section

### 4.1. Chemistry

All reagents and solvents were obtained from commercial suppliers and used without further purification unless otherwise indicated. Anhydrous solvents were dried and purified by conventional methods prior to use. Column chromatography was carried out on silica gel (200-300 mesh). All reactions were monitored by thinlayer chromatography (TLC) on silica gel plates with fluorescence F-254 and visualized with UV light. $^1$H NMR and $^{13}$C NMR spectral data were recorded in DMSO-$d_6$ on a Bruker ARX-400 NMR or Bruker ARX-600 NMR spectrometer with TMS as an internal standard. High resolution accurate mass spectrometry determinations (HRMS) for all final target compounds were obtained on a Bruker Micromass Time of Flight mass spectrometer equipped with an electrospray ionization (ESI) detector.

*4.1. 1. General procedure for the synthesis of 5-(2-chloroacetyl)indolin-2-one derivatives (**8a-d**).*

5-(2-chloroacetyl)indolin-2-one derivatives (**8a-d**) were synthesized according to previously reported methods[38].

*4.1.2. General procedure for the synthesis of 2-oxoindoline-5-carboxylic acid derivatives (**9a-d**).*

2-oxoindoline-5-carboxylic acid derivatives (**9a-d**) were synthesized according to previously reported methods[39].

*4.1.3. General procedure for the synthesis of compounds (**10a-n**).*

A solution of **9a-d** (2 mmol), EDCI (3 mmol) and HOBt (3 mmol) in dry DCM (20 mL) was stirred at 0 °C for 3.5 h. Then different substituted amines (2.2 mmol) and DIPEA (4 mmol) were added and the reaction was stirred at r.t. for another 1.5 h. The organic layer was washed with water and brine and dried over $Na_2SO_4$. Removal of the solvent gave a residue that was purified by column chromatography (silica gel, $CH_2Cl_2$-MeOH 100 : 1 as an eluent) to furnish **10a-n** as white solids.

*4.1.4. General procedure for the synthesis of target compounds (**11a-n,12a-g**).*

To a solution of **10a-n** (1.0 mmol) in ethanol (4 mL) was added the corresponding aldehydes (1.1 mmol) and

a catalytic amount of piperidine. The reaction mixture was stirred at reflux for 4.0 h (reaction monitored by TLC). After cooling, the precipitate was filtered, washed with cold ethanol, and dried in air to provide the title compounds **11a-n**, **12a-g** as brown yellow/brown/orange solids in moderate to excellent yields.

*4.1.4.1.(3Z)-N-[(1R)-2-hydroxy-1-phenylethyl]-3-(1H-pyrrol-2-ylmethylidene)-2-oxoindoline-5-carboxamide (**11a**).* Yellow solid, yield 83%; m.p.:251.5-253.0 °C; 1H NMR (400 MHz, DMSO) δ 13.28 (s, 1H), 11.15 (s, 1H), 8.53 (d, *J* = 8.0 Hz, 1H), 8.24 (s, 1H), 7.86-7.68 (m, 2H), 7.41 (d, *J* = 7.6 Hz, 3H), 7.33 (t, *J* = 7.5 Hz, 2H), 7.24 (d, *J* = 7.2 Hz, 1H), 7.02-6.82 (m, 2H), 6.39 (s, 1H), 5.10 (d, *J* = 5.9 Hz, 1H), 4.96 (t, *J* = 5.8 Hz, 1H), 3.79-3.60 (m, 2H). $^{13}$C NMR (151 MHz, DMSO) δ 170.02, 166.59, 142.06, 141.62, 129.96, 128.55, 128.20, 127.48, 127.45, 127.34, 127.22, 126.77, 125.30, 121.42, 118.18, 116.59, 112.20, 109.41, 65.08, 56.45. HRMS calcd for $C_{22}H_{19}N_3O_3$, $[M+H]^+$, 374.1499; found 374.1498.

*4.1.4.2. (3Z)-N-[(1S)-2-hydroxy-1-phenylethyl]-3-(1H-pyrrol-2-ylmethylidene)-2-oxoindoline-5-carboxamide (**11b**).* Yellow solid, yield 78%; m.p.:249.3-250.9 °C; $^1$H NMR (400 MHz, DMSO) δ 13.28 (s, 1H), 11.14 (s, 1H), 8.54 (d, *J* = 7.5 Hz, 1H), 8.24 (s, 1H), 7.87-7.68 (m, 2H), 7.41 (d, *J* = 7.3 Hz, 3H), 7.33 (t, *J* = 7.1 Hz, 2H), 7.24 (d, *J* = 6.9 Hz, 1H), 6.99-6.88 (m, 2H), 6.39 (s, 1H), 5.10 (d, *J* = 5.7 Hz, 1H), 4.96 (s, 1H), 3.81-3.60 (m, 2H). $^{13}$C NMR (151 MHz, DMSO) δ 169.58, 166.17, 141.59, 141.18, 129.52, 128.13, 127.81, 127.05, 126.98, 126.88, 126.81, 126.36, 124.86, 121.02, 117.68, 116.12, 111.78, 108.97, 99.56, 64.66, 55.94. HRMS calcd for $C_{22}H_{19}N_3O_3$, $[M+H]^+$, 374.1499; found 374.1503.

*4.1.4.3.(3Z)-N-[(1S)-1-(4-chlorophenyl)-2-hydroxyethyl]-3-(1H-pyrrol-2-ylmethylidene)-2-oxoindole-5-carboxamide (**11c**).* Yellow solid, yield 69%; m.p.:235.9-240.2 °C; $^1$H NMR (600 MHz, DMSO) δ 13.45 (s, 1H), 11.05 (s, 1H), 8.56 (dd, *J* = 19.8, 8.0 Hz, 1H), 8.22 (d, *J* = 8.1 Hz, 1H), 7.74 (dd, *J* = 17.0, 9.2 Hz, 2H), 7.38 (dq, *J* = 15.3, 8.1 Hz, 5H), 6.98-6.84 (m, 2H), 6.37 (s, 1H), 5.41-4.82 (m, 2H), 3.75-3.65 (m, 2H). $^{13}$C NMR (151 MHz, DMSO) δ 170.05, 166.23, 140.72, 131.33, 129.58, 129.38, 128.98, 128.10, 128.04, 127.31, 127.04, 126.89, 126.76, 126.66, 126.13, 125.07, 120.70, 117.62, 111.67, 109.10, 64.34, 55.37. HRMS calcd for $C_{22}H_{18}ClN_3O_3$, $[M+H]^+$, 408.1109; found 408.1112.

*4.1.4.4.(3Z)-N-[(1S)-1-(2-chlorophenyl)-2-hydroxyethyl]-3-(1H-pyrrol-2-ylmethylidene)-2-oxoindole-5-carboxamide (**11d**).* Yellow solid, yield 73%; m.p.:243.1-247.8 °C; $^1$H NMR (400 MHz, DMSO) δ 13.28 (s, 1H), 11.15 (s, 1H), 8.62 (d, *J* = 7.5 Hz, 1H), 8.26 (s, 1H), 7.83-7.73 (m, 2H), 7.58 (d, *J* = 7.5 Hz, 1H), 7.46-7.36 (m, 2H), 7.30 (ddd, *J* = 15.1, 11.8, 7.5 Hz, 2H), 6.99-6.89 (m, 2H), 6.39 (s, 1H), 5.48 (dd, *J* = 12.7, 7.5 Hz, 1H), 5.09 (t, *J* = 5.8 Hz, 1H), 3.83-3.52 (m, 2H). $^{13}$C NMR (151 MHz, DMSO) δ 170.01, 166.69, 141.70, 139.15, 132.66, 129.93, 129.62, 129.05, 128.79, 128.01, 127.68, 127.42, 127.38, 126.84, 125.30, 121.48, 118.14, 116.53, 112.24, 109.45, 63.38, 53.82. HRMS calcd for $C_{22}H_{18}ClN_3O_3$, $[M+H]^+$, 408.1109; found 408.1112.

*4.1.4.5.(3Z)-N-[(1S)-1-(4-fluorophenyl)-2-hydroxyethyl]-3-(1H-pyrrol-2-ylmethylidene)-2-oxoindole-5-carboxamide (**11e**).* Brown solid, yield 70%; m.p.:213.3-217.2 °C; $^1$H NMR (400 MHz, DMSO) δ 13.27 (s, 1H), 11.15 (s, 1H), 8.53 (d, *J* = 7.9 Hz, 1H), 8.22 (s, 1H), 7.75 (dd, *J* = 18.5, 11.7 Hz, 2H), 7.53-7.35 (m, 3H), 7.15 (t, *J* = 8.9 Hz, 2H), 6.98-6.89 (m, 2H), 6.39 (d, *J* = 3.4 Hz, 1H), 5.09 (dd, *J* = 13.6, 7.5 Hz, 1H), 5.00-4.91 (m, 1H), 3.76-3.59 (m, 2H). $^{13}$C NMR (151 MHz, DMSO) δ 170.53, 170.01, 166.81, 166.60, 162.44, 160.84, 144.37, 141.64, 138.32, 138.30, 138.22, 138.20, 130.13, 129.94, 129.43, 129.38, 128.15, 127.84, 127.43, 127.30, 126.82, 125.30, 122.10, 121.48, 118.75, 118.11, 116.52, 116.04, 115.33, 115.19, 112.22, 109.41, 64.93, 55.62, HRMS calcd for $C_{22}H_{17}FN_3O_3$, $[M+H]^+$, 392.1405; found 392.1409.

*4.1.4.6.(3Z)-N-[(2S)-1-hydroxy-3-phenylpropan-2-yl]-3-(1H-pyrrol-2-ylmethylidene)-2-oxoindoline-5-carboxamide (**11f**).* Brown solid, yield 68%; m.p.:211.1-215.9 °C; $^1$H NMR (400 MHz, DMSO) δ 13.26 (s, 1H), 11.12 (s, 1H), 8.12 (s, 1H), 8.02 (d, *J* = 8.4 Hz, 1H), 7.76 (s, 1H), 7.65 (dd, *J* = 8.1, 1.5 Hz, 1H), 7.40 (s, 1H), 7.35-7.21 (m, 4H), 7.16 (dd, *J* = 10.5, 4.2 Hz, 1H), 6.91 (d, *J* = 8.0 Hz, 2H), 6.38 (dd, *J* = 5.9, 2.3 Hz, 1H), 4.27 (t, *J* = 5.2 Hz, 1H), 4.23-4.13 (m, 1H), 3.47 (dtd, *J* = 16.7, 10.9, 5.7 Hz, 2H), 2.97 (dd, *J* = 13.7, 5.4 Hz,

1H), 2.82 (dd, *J* = 13.7, 8.8 Hz, 1H). $^{13}$C NMR (151 MHz, DMSO) δ 170.54, 169.99, 166.75, 166.40, 144.23, 141.49, 140.07, 139.99, 129.94, 129.54, 128.59, 128.54, 128.31, 128.19, 127.86, 127.31, 127.05, 126.78, 126.34, 125.25, 121.89, 121.44, 118.71, 118.02, 116.56, 116.06, 112.28, 112.18, 109.31, 109.12, 63.52, 63.45, 63.36, 53.81, 53.60, 41.95. HRMS calcd for $C_{23}H_{21}N_3O_3$, $[M+H]^+$, 388.1656; found 388.1660.

*4.1.4.7.(3Z)-N-[(2S)-1-hydroxy-3-methylbutan-2-yl]-3-(1H-pyrrol-2-ylmethylidene)-2-oxoindole-5-carboxamide* ***(11g)***. Yellow solid, yield 75%; m.p.:175.3-175.4 °C; $^1$H NMR (600 MHz, DMSO) δ 13.28 (s, 1H), 11.13 (s, 1H), 8.19 (d, *J* =1.4 Hz, 1H), 7.80 (t, *J* = 4.4 Hz, 2H), 7.72 (dt, *J* = 10.0, 5.0 Hz, 1H), 7.39 (d, *J* = 1.0 Hz, 1H), 6.97-6.88 (m, 2H), 6.39 (dq, *J* = 3.7, 2.7 Hz, 1H), 4.60 (t, *J* = 5.4 Hz, 1H), 3.83 (dq, *J* = 8.8, 5.5 Hz, 1H), 3.52 (dd, *J* = 12.3, 7.2 Hz, 2H), 2.00-1.87 (m, 1H), 0.92 (dd, *J* = 14.4, 6.8 Hz, 6H). $^{13}$C NMR (151 MHz, DMSO) δ 170.02, 166.78, 141.44, 129.96, 128.61, 127.36, 127.28, 126.70, 125.21, 121.35, 118.08, 116.67, 112.17, 109.32, 61.87, 56.99, 29.08, 20.20, 19.32. HRMS calcd for $C_{19}H_{21}N_3O_3$, $[M+H]^+$, 340.1656; found 340.1659.

*4.1.4.8.(3Z)-N-[(2S)-1-hydroxy-3,3-dimethylbutan-2-yl]-3-(1H-pyrrol-2-ylmethylidene)-2-oxoindole-5-carboxamid e* ***(11h)***. Brown solid, yield 80%; m.p.:215.4-220.6 °C; $^1$H NMR (600 MHz, DMSO) δ 13.29 (s, 1H), 11.12 (s, 1H), 8.19 (s, 1H), 7.88-7.79 (m, 1H), 7.71 (dd, *J* = 30.4, 8.5 Hz, 2H), 7.40 (s, 1H), 6.94 (d, *J* = 8.3 Hz, 2H), 6.39 (s, 1H), 4.46 (t, *J* = 5.5 Hz, 1H), 4.02-3.84 (m, 1H), 3.73-3.63 (m, 1H), 3.57-3.47 (m, 1H), 0.94 (s, 9H). $^{13}$C NMR (151 MHz, DMSO) δ 170.03, 167.30, 141.38, 129.96, 128.89, 127.37, 126.68, 125.16, 121.35, 118.15, 116.69, 112.17, 109.27, 60.90, 59.77, 34.61, 27.55. HRMS calcd for $C_{20}H_{23}N_3O_3$, $[M+H]^+$, 354.1812; found 354.1813.

*4.1.4.9.(3Z)-N-(2-hydroxyethyl)-3-(1H-pyrrol-2-ylmethylidene)-2-oxoindole-5-carboxamide* ***(11i)***. Yellow solid, yield 71%; m.p.:235.3-236.0 °C; $^1$H NMR (400 MHz, DMSO) δ 13.25 (s, 1H), 11.13 (s, 1H), 8.28 (t, *J* = 5.4 Hz, 1H), 8.17 (d, *J* = 1.1 Hz, 1H), 7.79 (s, 1H), 7.70 (dd, *J* = 8.2, 1.4 Hz, 1H), 7.39 (s, 1H), 6.91 (dd, *J* = 9.6, 4.9 Hz, 2H), 6.38 (dd, *J* = 5.8, 2.3 Hz, 1H), 4.74 (t, *J* = 5.6 Hz, 1H), 3.52 (q, *J* = 6.0 Hz, 2H), 3.38-3.33 (m, 2H). $^{13}$C NMR (151 MHz, DMSO) δ 170.00, 166.85, 141.52, 129.97, 128.21, 127.38, 126.96, 126.78, 125.34, 121.45, 118.04, 116.54, 112.17, 109.38, 60.38, 42.67. HRMS calcd for $C_{16}H_{15}N_3O_3$, $[M+H]^+$, 298.1186; found 298.1191.

*4.1.4.10.(3Z)-N-(2-hydroxypropyl)-3-(1H-pyrrol-2-ylmethylidene)-2-oxoindole-5-carboxamide* ***(11j)***. Yellow solid, yield 69%; m.p.:203.7-206.9 °C; $^1$H NMR (600 MHz, DMSO) δ 13.27 (s, 1H), 11.18 (s, 1H), 8.48-8.33 (m, 1H), 8.19 (s, 1H), 7.80 (s, 1H), 7.74-7.64 (m, 2H), 7.57 (s, 1H), 7.39 (s, 1H), 6.98-6.86 (m, 2H), 6.53-6.30 (m, 1H), 4.55 (s, 1H), 3.51-3.42 (m, 3H), 3.32-3.28 (m, 2H). $^{13}$C NMR (151 MHz, DMSO) δ 170.05, 166.23, 140.72, 131.33, 129.58, 129.38, 128.98, 128.10, 128.04, 127.31, 127.04, 126.89, 126.76, 126.66, 126.13, 125.07, 120.70, 117.62, 111.67, 109.10, 64.34, 55.37. HRMS calcd for $C_{17}H_{17}N_3O_3$, $[M+H]^+$, 312.1343; found 312.1347.

*4.1.4.11. (3Z)-N-[(1R)-3-hydroxy-1-phenylpropyl]-3-(1H-pyrrol-2-ylmethylidene)-2-oxoindole-5-carboxamide* ***(11k)***. Yellow solid, yield 83%; m.p.:258.9-261.8 °C; $^1$H NMR (600 MHz, DMSO) δ 13.27 (s, 1H), 11.14 (s, 1H), 8.81-8.50 (m, 1H), 8.18 (d, *J* = 1.2 Hz, 1H), 7.79 (s, 1H), 7.73 (ddd, *J* = 23.8, 8.1, 1.5 Hz, 1H), 7.40 (d, *J* = 7.2 Hz, 3H), 7.33 (t, *J* = 7.7 Hz, 2H), 7.22 (t, *J* = 7.3 Hz, 1H), 6.96-6.89 (m, 2H), 6.50-6.33 (m, 1H), 5.18 (d, *J* = 6.0 Hz, 1H), 4.57 (t, *J* = 4.9 Hz, 1H), 3.54-3.37 (m, 2H), 1.99 (ddd, *J* = 20.0, 10.7, 5.8 Hz, 2H). $^{13}$C NMR (151 MHz, DMSO) δ 169.56, 165.86, 144.35, 141.14, 129.50, 128.22, 127.82, 127.01, 126.73, 126.56, 126.35, 124.88, 121.05, 117.60, 116.06, 111.75, 108.95, 57.97, 50.23. HRMS calcd for $C_{23}H_{21}N_3O_3$, $[M+H]^+$, 388.1656; found 388.1659.

*4.1.4.12. (3Z)-6-fluoro-N-[(1S)-2-hydroxy-1-phenylethyl]-3-(1H-pyrrol-2-ylmethylidene)-2-oxoindole-5-carboxamide* ***(11l)***. Yellow solid, yield 67%; m.p.:164.7-168.6 °C; $^1$H NMR (400 MHz, DMSO) δ 13.11 (s, 1H), 11.23 (s, 1H), 8.42 (dd, *J* = 7.7, 2.9 Hz, 1H), 7.94 (d, *J* = 7.0 Hz, 1H), 7.87 (s, 1H), 7.40 (d, *J* = 7.6 Hz, 3H), 7.33 (t, *J* = 7.5 Hz, 2H), 7.25 (d, *J* = 7.1 Hz, 1H), 6.88 (s, 1H), 6.76 (dd, *J* = 10.7, 5.3 Hz, 1H), 6.39 (t, *J* = 12.6 Hz, 1H), 5.06-4.94 (m, 2H), 3.67 (t, *J* = 5.5 Hz, 2H). $^{13}$C NMR (151 MHz, DMSO) δ 169.53, 169.01, 162.99, 162.75, 159.33, 158.41, 157.69, 144.40, 144.31, 140.93, 140.85, 140.69, 140.60, 128.89, 127.55, 127.50, 126.72, 126.61, 126.35, 126.26, 126.19, 125.73, 125.14, 124.30, 122.79, 120.72, 120.56, 119.32, 119.30, 117.53, 116.66, 116.15, 116.05, 115.14, 115.05, 114.72, 114.30, 111.17, 111.07, 97.16, 96.97, 64.02, 55.18, 55.08. HRMS calcd for

$C_{22}H_{18}ClN_3O_3$, $[M+H]^+$, 408.1109; found 408.1112.

*4.1.4.13.(3Z)-6-chloro-N-[(1S)-2-hydroxy-1-phenylethyl]-3-(1H-pyrrol-2-ylmethylidene)-2-oxoindole-5-carboxamide (**11m**)*. Yellow solid, yield 71%; m.p.:281.0-283.8 °C; $^1$H NMR (400 MHz, DMSO) δ 13.20 (s, 1H), 11.13 (s, 1H), 8.69 (d, *J* = 8.1 Hz, 1H), 7.92 (s, 1H), 7.78 (s, 1H), 7.42 (d, *J* = 7.5 Hz, 3H), 7.34 (t, *J* = 7.5 Hz, 2H), 7.25 (t, *J* = 7.2 Hz, 1H), 6.91 (d, *J* = 7.4 Hz, 2H), 6.42-6.36 (m, 1H), 4.94 (dt, *J* = 11.6, 6.3 Hz, 2H), 3.70-3.59 (m, 2H). $^{13}$C NMR (151 MHz, DMSO) δ 169.34, 166.28, 141.06, 140.08, 129.87, 129.58, 128.11, 128.02, 128.00, 127.19, 126.85, 126.81, 124.01, 121.56, 119.04, 114.99, 111.92, 110.16, 64.80, 55.88. HRMS calcd for $C_{22}H_{18}ClN_3O_3$, $[M+H]^+$, 408.1109; found 408.1114.

*4.1.4.14. (3Z)-6-bromo-N-[(1S)-2-hydroxy-1-phenylethyl]-3-(1H-pyrrol-2-ylmethylidene)-2-oxoindole-5-carboxamide (**11n**)*. Brown solid, yield 59%; m.p.:276.7-280.8 °C; $^1$H NMR (600 MHz, DMSO) δ 13.21 (s, 1H), 11.11 (s, 1H), 8.69 (d, *J* = 8.2 Hz, 1H), 7.93 (s, 1H), 7.75 (s, 1H), 7.43 (dd, *J* = 8.1, 5.0 Hz, 3H), 7.35 (t, *J* = 7.7 Hz, 2H), 7.26 (t, *J* = 7.3 Hz, 1H), 7.07 (s, 1H), 6.91 (d, *J* = 1.6 Hz, 1H), 6.39 (dt, *J* = 3.7, 2.3 Hz, 1H), 5.02 (dd, *J* = 14.2, 7.2 Hz, 1H), 4.87 (t, *J* = 5.9 Hz, 1H), 3.71-3.61 (m, 2H). $^{13}$C NMR (151 MHz, DMSO) δ 169.56, 165.86, 144.35, 141.14, 129.50, 128.22, 127.82, 127.01, 126.73, 126.56, 126.35, 124.88, 121.05, 117.60, 116.06, 111.75, 108.95, 57.97, 50.23. HRMS calcd for $C_{22}H_{18}BrN_3O_3$, $[M+H]^+$, 452.0604; found 452.0603.

*4.1.4.15.(3E)-3-(furan-2-ylmethylidene)-N-[(1S)-2-hydroxy-1-phenylethyl]-2-oxoindole-5-carboxamide (**12a**)*. Yellow solid, yield 87%; m.p.:281.7-284.2 °C; $^1$H NMR (400 MHz, DMSO) δ 10.83 (s, 1H), 8.87 (s, 1H), 8.64 (d, *J* = 8.0 Hz, 1H), 8.08 (s, 1H), 7.84 (d, *J* = 8.2 Hz, 1H), 7.41 (d, *J* = 9.4 Hz, 3H), 7.33 (dd, *J* = 9.2, 5.5 Hz, 3H), 7.24 (t, *J* = 7.2 Hz, 1H), 6.93 (d, *J* = 8.2 Hz, 1H), 6.84 (dd, *J* = 3.3, 1.7 Hz, 1H), 5.07 (dd, *J* = 13.5, 7.8 Hz, 1H), 4.93 (t, *J* = 5.8 Hz, 1H), 3.75-3.63 (m, 2H). $^{13}$C NMR (151 MHz, DMSO) δ 170.04, 166.84, 151.04, 147.84, 145.25, 142.19, 129.62, 128.76, 128.58, 127.47, 127.26, 124.79, 122.01, 121.97, 121.44, 120.60, 114.26, 109.37, 65.16, 56.48. HRMS calcd for $C_{22}H_{18}N_2O_4$, $[M+H]^+$, 375.1339; found 375.1344.

*4.1.4.16. (3Z)-N-[(1S)-2-hydroxy-1-phenylethyl]-3-(thiophen-2-ylmethylidene)-2-oxoindole-5-carboxamide (**12b**)*. Yellow solid, yield 85%; m.p.:255.2-258.4 °C; $^1$H NMR (400 MHz, DMSO) δ 10.88 (s, 1H), 8.59 (dd, *J* = 47.8, 8.0 Hz, 1H), 8.27 (s, 1H), 8.18 (s, 1H), 8.02 (dd, *J* = 18.0, 4.0 Hz, 1H), 7.96-7.76 (m, 2H), 7.46-7.18 (m, 6H), 6.94 (dd, *J* = 20.9, 8.1 Hz, 1H), 5.19-4.83 (m, 2H), 3.80-3.58 (m, 2H). $^{13}$C NMR (151 MHz, DMSO) δ 170.05, 166.23, 140.72, 131.33, 129.58, 129.38, 128.98, 128.10, 128.04, 127.31, 127.04, 126.89, 126.76, 126.66, 126.13, 125.07, 120.70, 117.62, 111.67, 109.10, 64.34, 55.37. HRMS calcd for $C_{22}H_{18}N_2O_3S$, $[M+H]^+$, 391.1111; found 391.1110.

*4.1.4.17.(3E)-N-[(1S)-2-hydroxy-1-phenylethyl]-3-(pyridin-2-ylmethylidene)-2-oxoindole-5-carboxamide (**12c**)*. Brown solid, yield 90%; m.p.:262.4-265.6℃; $^1$H NMR (400 MHz, DMSO) δ 10.89 (s, 1H), 9.56 (d, *J* = 1.2 Hz, 1H), 8.85 (d, *J* = 4.2 Hz, 1H), 8.54 (d, *J* = 8.0 Hz, 1H), 8.08-7.79 (m, 3H), 7.64 (s, 1H), 7.51 (dd, *J* = 6.8, 5.3 Hz, 1H), 7.42 (d, *J* = 7.4 Hz, 2H), 7.34 (t, *J* = 7.5 Hz, 2H), 7.25 (t, *J* = 7.2 Hz, 1H), 6.93 (d, *J* = 8.1 Hz, 1H), 5.20-4.86 (m, 2H), 3.90-3.52 (m, 2H). $^{13}$C NMR (151 MHz, DMSO) δ 169.62, 166.48, 153.03, 149.72, 145.86, 141.74, 137.41, 134.66, 130.45, 128.82, 128.65, 128.37, 128.15, 127.75, 127.03, 126.83, 124.48, 121.16, 109.01, 64.74, 55.86. HRMS calcd for $C_{23}H_{19}N_3O_3$, $[M+H]^+$, 386.1499; found 386.1506.

*4.1.4.18.(3Z)-N-[(1S)-2-hydroxy-1-phenylethyl]-3-(3H-imidazol-4-ylmethylidene)-2-oxoindole-5-carboxamide (**12d**)*. Yellow solid, yield 70%; m.p.:199.8-204.1 °C; $^1$H NMR (600 MHz, DMSO) δ 13.59 (s, 1H), 11.78 (s, 1H), 8.59 (d, 1H), 8.49-8.21 (m, 1H), 7.95 (dd, 2H), 7.76 (dd, 1H), 7.41 (d, 2H), 7.33 (dd, 2H), 7.23 (t, 1H), 6.90 (dd, 1H), 5.07 (ddd,2H), 3.70 (dt, 2H). $^{13}$C NMR (151 MHz, DMSO) δ 170.32, 166.91, 165.95, 143.80, 142.13, 141.88, 141.56, 138.65, 129.40, 128.15, 128.13, 128.11, 128.02, 127.71, 127.03, 127.01, 126.81, 126.75, 126.50, 124.21, 122.48, 120.55, 115.23, 109.15, 108.00, 69.80, 64.79, 64.65, 55.96, 55.78. HRMS calcd for $C_{23}H_{19}N_3O_3$, $[M+H]^+$, 386.1499; found 386.1506. HRMS calcd for $C_{21}H_{18}N_4O_3$, $[M+H]^+$, 375.1452; found 375.1470.

*4.1.4.19.(3Z)-N-[(1S)-2-hydroxy-1-phenylethyl]-3-(1H-imidazol-2-ylmethylidene)-2-oxoindole-5-carboxamide (**12e**)*. Yellow solid, yield 76%; m.p.:208.3-212.8 °C; $^1$H NMR (600 MHz, DMSO) δ 13.98 (s, 1H), 10.87 (s, 1H),

9.87 (d, *J* = 1.2 Hz, 1H), 8.92-8.38 (m, 1H), 7.97-7.78 (m, 1H), 7.59 (s, 1H), 7.49-7.36 (m, 4H), 7.32 (dd, *J* = 12.8, 7.3 Hz, 2H), 7.23 (dd, *J* = 11.7, 7.2 Hz, 1H), 6.96 (dd, *J* = 56.3, 8.1 Hz, 1H), 5.30-4.92 (m, 2H), 3.92-3.54 (m, 2H). $^{13}$C NMR (151 MHz, DMSO) δ 170.26, 169.71, 167.13, 166.06, 145.16, 143.95, 143.32, 142.74, 142.31, 142.04, 141.03, 133.32, 129.66, 129.33, 129.00, 128.86, 128.63, 128.60, 128.54, 128.52, 128.42, 127.62, 127.45, 127.17, 125.35, 124.62, 124.09, 123.50, 122.10, 121.76, 121.61, 119.55, 118.72, 118.46, 110.08, 108.78, 71.69, 65.16, 65.09, 56.64, 56.46, 56.37, 48.40, 48.18. HRMS calcd for $C_{21}H_{18}N_4O_3$, $[M+H]^+$, 375.1452; found 375.1457.

*4.1.4.20.(3Z)-N-[(1S)-2-hydroxy-1-phenylethyl]-3-(2H-pyrazol-3-ylmethylidene)-2-oxoindole-5-carboxamide (**12f**).* Brown solid, yield 77%; m.p.:251.9-255.5 °C; $^1$H NMR (600 MHz, DMSO) δ 13.67 (s, 1H), 10.81 (s, 1H), 8.53 (m, 2H), 7.97-7.73 (m, 2H), 7.58 (d, 1H), 7.32 (tt, *J* = 13.0, 7.6 Hz, 5H), 6.90 (m, 2H), 5.05 (m, 2H), 3.81-3.53 (m, 2H). $^{13}$C NMR (151 MHz, DMSO) δ 170.27, 167.06, 166.25, 145.19, 142.29, 141.96, 129.51, 129.36, 128.83, 128.59, 128.56, 127.50, 127.46, 127.27, 127.20, 124.85, 122.17, 108.78, 65.12, 65.10, 56.56, 56.41. HRMS calcd for $C_{21}H_{18}N_4O_3$, $[M+H]^+$, 375.1452; found 375.1477.

*4.1.4.21.(3Z)-3-[(3,5-dimethyl-1H-pyrrol-2-yl)methylidene]-N-[(1S)-2-hydroxy-1-phenylethyl]-2-oxoindoline-5-carboxamide (**12g**).* Orange solid, yield 85%; m.p.:274.3-275.5 °C; $^1$H NMR (400 MHz, DMSO) δ 13.34 (s, 1H), 11.07 (s, 1H), 8.74 (d, *J* = 7.4 Hz, 1H), 8.52 (s, 1H), 7.80-7.67 (m, 2H), 7.40 (d, *J* = 7.4 Hz, 2H), 7.31 (t, *J* = 7.5 Hz, 2H), 7.22 (t, *J* = 7.2 Hz, 1H), 6.92 (d, *J* = 8.1 Hz, 1H), 6.04 (s, 1H), 5.17 (t, *J* = 6.0 Hz, 1H), 5.05 (dd, *J* = 12.7, 7.3 Hz, 1H), 3.84-3.63 (m, 2H), 2.35 (d, *J* = 9.2 Hz, 6H). $^{13}$C NMR (151 MHz, DMSO) δ 170.22, 166.69, 142.29, 140.69, 136.79, 133.04, 128.44, 127.66, 127.49, 127.32, 127.05, 126.27, 126.06, 124.86, 117.98, 113.26, 112.45, 109.06, 64.96, 56.85, 14.05, 12.05. HRMS calcd for $C_{24}H_{23}N_3O_3$, $[M+H]^+$, 402.1812; found 402.1816.

*4.1.5.(3Z)-6-cyano-N-[(1S)-2-hydroxy-1-phenylethyl]-3-(1H-pyrrol-2-ylmethylidene)-2-oxoindoline-5-carboxamide (**11o**)*

A mixture of **11n** (1.0 mmol), zinc cyanide (2.0 mmol), $Pd(P(Ph_3)_4)$ (0.1 mmol) in DMF was heated at 185 °C for 10 h. The reaction mixture was cooled to room temperature, diluted with ethyl acetate and filtered. The filtrate was concentrated *in vacuo*, and the residue purified by column chromatography (silica gel, $CH_2Cl_2$-MeOH 100:1 as an eluent). The product was obtained as an orange solid, yield 54%; m.p.:205.7-207.6 °C. $^1$H NMR (400 MHz, DMSO) δ 13.30 (s, 1H), 10.08 (s, 1H), 8.15 (s, 1H), 8.09 (s, 1H), 7.68 (s, 1H), 7.47 (s, 1H), 7.40 (d, *J* = 7.4 Hz, 2H), 7.31 (t, *J* = 7.5 Hz, 2H), 7.23 (t, *J* = 7.3 Hz, 1H), 6.96 (s, 1H), 6.42 (s, 1H), 5.56 (dd, *J* = 8.5, 5.8 Hz, 1H), 5.14 (t, *J* = 5.7 Hz, 1H), 4.46 (ddd, *J* = 22.6, 12.8, 7.5 Hz, 2H), 4.08 (dt, *J* = 11.1, 5.5 Hz, 1H). $^{13}$C NMR (151 MHz, DMSO) δ 169.86, 168.77, 160.01, 143.08, 139.45, 130.45, 130.25, 129.99, 129.75, 128.70, 128.16, 127.97, 127.52, 124.31, 123.02, 115.42, 113.11, 112.73, 104.02, 72.98, 63.51, 63.25, 61.19, 56.95. HRMS calcd for $C_{23}H_{18}N_4O_3$ $[M+H]^+$, 399.1452; found 399.1455.

*4.1.6. General procedure for the synthesis of target compounds (**11p-q**)*

A solution of **11n** (1.0 mmol) in toluene : ethanol (volume 4:1,10 mL) was degassed by $N_2$ bubbling for 5 min. The corresponding boronic acid/ester (1.5 mmol) was added and the mixture was degassed for another 5 min. $Pd(P(Ph_3)_4)$ (0.1 mol) and aqueous potassium carbonate (2 M, 3.0 eq.) were added sequentially and the mixture was further degassed for 5 min and then heated at 110 °C for 16 h. The mixture was quenched with water and extracted with ethyl acetate (3 × 50 mL). The combined organic layer was washed with water, brine and dried over sodium sulphate. The solvent was distilled off under reduced pressure, and the crude residue was purified by column chromatography to yield the product.

*4.1.6.1.(3Z)-N-[(1S)-2-hydroxy-1-phenylethyl]-6-(2-methylpyrazol-3-yl)-3-(1H-pyrrol-2-ylmethylidene)-2-oxoindole-5-carboxamide (**11p**).* Yellow solid, yield 59%; m.p.:136.5-140.2 °C; $^1$H NMR (400 MHz, DMSO) δ 13.31 (s, 1H), 11.25 (s, 1H), 8.59 (m, 1H), 7.93 (m, 2H), 7.46-7.18 (m, 7H), 6.95 (s, 1H), 6.80 (s, 1H), 6.40 (s, 1H), 6.18 (d, *J* = 1.6 Hz, 1H), 5.02-4.79 (m, 2H), 3.66-3.54 (m, 1H), 3.52 (d, *J* = 11.5 Hz, 3H), 3.39 (s, 1H). $^{13}$C NMR (151 MHz, DMSO) δ 169.43, 167.75, 141.81, 141.06, 139.52, 137.43, 130.80, 129.67, 128.07, 128.05, 128.01, 127.25,

127.11, 127.08, 126.75, 126.71, 125.33, 121.50, 118.39, 115.56, 111.93, 111.57, 106.39, 72.57, 64.74, 64.57, 63.05, 62.83, 55.90, 36.68. HRMS calcd for $C_{26}H_{23}N_5O_3$ $[M+H]^+$, 454.1874; found 454.1877.

*4.1.6.2.(3Z)-N-[(1S)-2-hydroxy-1-phenylethyl]-6-(1-methylpyrazol-4-yl)-3-(1H-pyrrol-2-ylmethylidene)-2-oxoindole-5-carboxamide (**11q**)*. Yellow solid, yield 47%; m.p.:285.6-288.4 °C; $^1$H NMR (400 MHz, DMSO) δ 13.25 (s, 1H), 11.02 (s, 1H), 8.72 (d, *J* = 8.3 Hz, 1H), 7.82 (s, 1H), 7.68 (s, 1H), 7.58 (d, *J* = 14.6 Hz, 2H), 7.32 (dt, *J* = 8.3, 5.0 Hz, 6H), 6.90 (d, *J* = 18.4 Hz, 2H), 6.36 (d, *J* = 3.1 Hz, 1H), 5.11-4.89 (m, 2H), 3.86-3.42 (m, 5H). $^{13}$C NMR (151 MHz, DMSO) δ 170.10, 141.46, 139.96, 137.82, 130.28, 130.13, 129.60, 129.18, 128.62, 127.67, 127.34, 127.03, 126.41, 123.26, 121.13, 120.71, 118.39, 116.60, 112.04, 108.89, 65.23, 56.16, 38.91. HRMS calcd for $C_{26}H_{23}N_5O_3$ $[M+H]^+$, 454.1874; found 454.1870.

## 4.2. **Pharmacological assay**

### 4.2.1. *PAK4 HTRF Assays.*

HTRF assays were performed in white 384 Well Small Volume plates with a total working volume of 20 µL. Compounds were dispensed, with 4 µL per well, from a concentration stock of 20 mM in 100% DMSO and with serial kinase reaction buffer dilutions. The $IC_{50}$ measurements were performed in replicates. All HTRF reagents were purchased from CisBio Bioassays and reconstituted according to the supplier protocols. For each assay 6 µL of mix 1 (kinase + ATP + substrate S2) is added in the assay wells, containing previously dispensed inhibitors. The assay wells were incubated at R.T. for 60 min, and terminated by adding 10 µL of mix 2 (Sa-XL665 + STK-Antibody-Cryptate). After a final incubation (60 min at room temperature), HTRF signal was obtained by reading the plate in Infinite® F500 microplate reader (Tecan, Switzerland). The fluorescence is measured at 620 nM (Cryptate) and 665 nM (XL665). A ratio is calculated (665/620) for each well. For $IC_{50}$ measurements, values were normalized and fitted with Prism (GraphPad software) using the following equation: Y = 100 / (1 + ((X / $IC_{50}$)^Hill slope)).

### 4.2.2. *Cell Proliferation Assay.*

Cells were seeded in 96-well cell culture plates. On the day of seeding, the cells were exposed to various concentrations of compounds and further cultured for 72 h at 37 °C. Cell proliferation was then determined using Cell Counts Kit-8 (CCK8) assay. The $IC_{50}$ values were calculated by a concentration-response curve fitting using the four-parameter method.

### 4.2.3. *Cell-cycle analysis by flow cytometry.*

A549 cells ($5\times10^5$ cells) were incubated with the indicated concentrations of **12g** for 72 h. After incubation, cells were collected, washed with PBS, and suspended in a staining buffer (10 µg/mL propidium iodide, 0.5% Tween-20, 0.1% RNase in PBS). The cells were analysed using a FACSVantage flow cytometer with the Cell Quest acquisition and analysis software program (Becton Dickinson and Co., San Jose, CA).

### 4.2.4. *Cell Migration and Invasion Assay.*

Cell migration assays were evaluated in Transwell chambers (Corning Costar). Cell invasion assays were evaluated in Matrigel invasion chambers (Corning Costar). Then, $5 \times 10^5$ cells in 100 µL serum-free DMEM supplemented with 0.1% bovine serum were placed in the upper part of each chamber and the lower compartments were filled with 600 µL DMEM containing 10% serum. After incubation for 24 h at 37 °C, the cells were fixed in 100% methanol and stained with 0.25% crystal violet; the cells that had not migrated or non-invaded from the top surface of the filters were removed with cotton. Invaded/migrated cells were quantitated by counting cells in six randomly selected fields on each filter under a microscope at 200 × magnification and graphed as the mean of three independent experiments.

### 4.2.5. *Western Blot Analysis.*

A549 cells were treated with the indicated dose of **12g** for 2 h and then lysed in 1x sodium dodecyl sulphate (SDS) sample buffer. The cell lysates were subsequently resolved by 10% SDS-PAGE and transferred to

nitrocellulose membranes. The membranes were probed with the appropriate primary antibodies [phospho-PAK4, PAK4, phospho-LIMK, LIMK, phospho-Cofilin, Cofilin, GAPDH (all from KeyGEN BioTECH, Nanjing,China)], and then with horseradish peroxidase-conjugated antirabbit or antimouse IgG. The immunoreactive proteins were detected using an enhanced chemiluminescence detection reagent (Thermo Fisher Scientific, Rockford, IL, USA).

5.3. *Molecular docking study.*

X-ray protein structure of PAK4 (PDB ID : 2X4Z) obtained from the Protein Data Bank was prepared with AutoDockTools (ADT). Both the native ligand and the indicated compounds were built using 2D Sketcher and were prepared with LigPrep with OPLS2005 force field, generating possible states at pH 7.0 ± 2.0 using Epik 2.0 module. The size of box was set to 60 × 60 × 60 units in number of grid points and grid spacing = 0.375 Å centred in native ligand using AutoGrid4. Docking was performed using the Lamarckian genetic algorithm in AutoDock4. Each docking experiment was performed 10 times, yielding 10 docked conformations and the most favourable pose of **12g** was displayed.

**Acknowledgments.**

We gratefully acknowledge the financial support from the National Natural Science Foundation of China (Grant 81230077) and Program for Innovative Research Team of the Ministry of Education, and Program for Liaoning Innovative Research Team in University.

**Appendix A. Supplementary data**

Supplementary data associated with this article can be found in the online version.

**References**

1. Callow, M. G.; Clairvoyant, F.; Zhu, S.; Schryver, B.; Whyte, D. B.; Bischoff, J. R.; Jallal, B.; Smeal, T. *Journal of Biological Chemistry* **2002,** *277*, 550.

2. Callow, M. G.; Zozulya, S.; Gishizky, M. L.; Jallal, B.; Smeal, T. *Journal of Cell Science* **2005,** *118*, 1861.

3. Cammarano, M. S.; Nekrasova, T.; Noel, B.; Minden, A. *Molecular and Cellular Biology* **2005,** *25*, 9532.

4. Liu, Y.; Xiao, H.; Tian, Y.; Nekrasova, T.; Hao, X.; Lee, H. J.; Suh, N.; Yang, C. S.; Minden, A. *Mol Cancer Res* **2008,** *6*, 1215.

5. Kumar, R.; Gururaj, A. E.; Barnes, C. J. *Nature Reviews Cancer* **2006,** *6*, 459.

6. Zhao, Z. S.; Manser, E. *Cell Logist* **2012,** *2*, 59.

7. Zhou, W.; Jubb, A. M.; Lyle, K.; Xiao, Q.; Ong, C. C.; Desai, R.; Fu, L.; Gnad, F.; Song, Q.; Haverty, P. M.; Aust, D.; Grutzmann, R.; Romero, M.; Totpal, K.; Neve, R. M.; Yan, Y.; Forrest, W. F.; Wang, Y.; Raja, R.; Pilarsky, C.; de Jesus-Acosta, A.; Belvin, M.; Friedman, L. S.; Merchant, M.; Jaffee, E. M.; Zheng, L.; Koeppen, H.; Hoeflich, K. P. *J Pathol* **2014,** *234*, 502.

8. Rudolph, J.; Murray, L. J.; Ndubaku, C. O.; O'Brien, T.; Blackwood, E.; Wang, W. R.; Aliagas, I.; Gazzard, L.; Crawford, J. J.; Drobnick, J.; Lee, W. D.; Zhao, X. R.; Hoeflich, K. P.; Favor, D. A.; Dong, P.; Zhang, H. M.; Heise, C. E.; Oh, A.; Ong, C. C.; La, H.; Chakravarty, P.; Chan, C.; Jakubiak, D.; Epler, J.; Ramaswamy, S.; Vega, R.; Cain, G.; Diaz, D.; Zhong, Y. *Journal of Medicinal Chemistry* **2016,** *59*, 5520.

9. Murray, B. W.; Guo, C.; Piraino, J.; Westwick, J. K.; Zhang, C.; Lamerdin, J.; Dagostino, E.; Knighton, D.; Loi, C. M.; Zager, M.; Kraynov, E.; Popoff, I.; Christensen, J. G.; Martinez, R.; Kephart, S. E.; Marakovits, J.; Karlicek, S.; Bergqvist, S.; Smeal, T. *Proc Natl Acad Sci U S A* **2010,** *107*, 9446.

10. Roth, G. J.; Binder, R.; Colbatzky, F.; Dallinger, C.; Schlenker-Herceg, R.; Hilberg, F.; Wollin, S. L.; Kaiser, R. *Journal of Medicinal Chemistry* **2015,** *58*, 1053.

11. Staben, S. T.; Feng, J. A.; Lyle, K.; Belvin, M.; Boggs, J.; Burch, J. D.; Chua, C. C.; Cui, H.; DiPasquale, A. G.; Friedman, L. S.; Heise, C.; Koeppen, H.; Kotey, A.; Mintzer, R.; Oh, A.; Roberts, D. A.; Rouge, L.; Rudolph, J.; Tam, C.; Wang, W.; Xiao, Y.; Young, A.; Zhang, Y.; Hoeflich, K. P. *J Med Chem* **2014,** *57*, 1033.

12. Mitchell, S.; Orwick, S.; Cannon, M.; Goettl, V. M.; LaFollette, T. D.; Baloglu, E.; Senapedis, W.; Walker, A.

R.; Bhatnagar, B.; Mims, A. S.; Klisovic, R. B.; Vasu, S.; Blum, W.; Lucas, D. M.; Blachly, J. S.; Garzon, R.; Bloomfield, C. D.; Lapalombella, R.; Byrd, J. C. *Blood* **2015,** *126*.

13. Omran Abu Aboud, C.-H. C., William Senapedis, Erkan Baloglu, Christian Argueta and Robert H. Weiss. *Molecular Cancer Therapeutics* **2016**.

14. Clinicaltrials.gov; *NCT*02702492.

15. Ryu, B. J.; Kim, S.; Min, B.; Kim, K. Y.; Lee, J. S.; Park, W. J.; Lee, H.; Kim, S. H.; Park, S. *Cancer Letters* **2014,** *349*, 45.

16. Hao, C.; Huang, W.; Li, X.; Guo, J.; Chen, M.; Yan, Z.; Wang, K.; Jiang, X.; Song, S.; Wang, J.; Zhao, D.; Li, F.; Cheng, M. *European Journal of Medicinal Chemistry* **2017,** *131*, 1.

17. Kaur, M.; Singh, M.; Chadha, N.; Silakari, O. *European Journal of Medicinal Chemistry* **2016,** *123*, 858.

18. Cui, J. J.; McTigue, M.; Nambu, M.; Tran-Dube, M.; Pairish, M.; Shen, H.; Jia, L.; Cheng, H. M.; Hoffman, J.; Le, P.; Jalaie, M.; Goetz, G. H.; Koenig, M.; Vojkovsky, T.; Zhang, F. J.; Do, S.; Botrous, I.; Ryan, K.; Grodsky, N.; Deng, Y. L.; Parker, M.; Timofeevski, S.; Murray, B. W.; Yamazaki, S.; Aguirre, S.; Li, Q. H.; Zou, H.; Christensen, J. *Journal of Medicinal Chemistry* **2012,** *55*, 10314.

19. Haddach, M.; Michaux, J.; Schwaebe, M. K.; Pierre, F.; O'Brien, S. E.; Borsan, C.; Tran, J.; Raffaele, N.; Ravula, S.; Drygin, D.; Siddiqui-Jain, A.; Darjania, L.; Stansfield, R.; Proffitt, C.; Macalino, D.; Streiner, N.; Bliesath, J.; Omori, M.; Whitten, J. P.; Anderes, K.; Rice, W. G.; Ryckman, D. M. *Acs Medicinal Chemistry Letters* **2012,** *3*, 135.

20. Jagtap, A. D.; Chang, P. T.; Liu, J. R.; Wang, H. C.; Kondekar, N. B.; Shen, L. J.; Tseng, H. W.; Chen, G. S.; Chern, J. W. *European Journal of Medicinal Chemistry* **2014,** *85*, 268.

21. Wang, H. C.; Jagtap, A. D.; Chang, P. T.; Liu, J. R.; Liu, C. P.; Tseng, H. W.; Chen, G. S.; Chern, J. W. *European Journal of Medicinal Chemistry* **2014,** *84*, 312.

22. Pergola, C.; Gaboriaud-Kolar, N.; Jestadt, N.; Konig, S.; Kritsanida, M.; Schaible, A. M.; Li, H. K.; Garscha, U.; Weinigel, C.; Barz, D.; Albring, K. F.; Huber, O.; Skaltsounis, A. L.; Werz, O. *Journal of Medicinal Chemistry* **2014,** *57*, 3715.

23. Sampson, P. B.; Liu, Y.; Patel, N. K.; Feher, M.; Forrest, B.; Li, S. W.; Edwards, L.; Laufer, R.; Lang, Y. H.; Ban, F. Q.; Awrey, D. E.; Mao, G. D.; Plotnikova, O.; Leung, G.; Hodgson, R.; Mason, J.; Wei, X.; Kiarash, R.; Green, E.; Qiu, W.; Chirgadze, N. Y.; Mak, T. W.; Pan, G. H.; Pauls, H. W. *Journal of Medicinal Chemistry* **2015,** *58*, 130.

24. Eswaran, J.; Lee, W. H.; Debreczeni, J. E.; Filippakopoulos, P.; Turnbull, A.; Fedorov, O.; Deacon, S. W.; Peterson, J. R.; Knapp, S. *Structure* **2007,** *15*, 201.

25. Gao, J.; Ha, B. H.; Lou, H. J.; Morse, E. M.; Zhang, R.; Calderwood, D. A.; Turk, B. E.; Boggon, T. J. *Plos One* **2013,** *8*.

26. Senwar, K. R.; Reddy, T. S.; Thummuri, D.; Sharma, P.; Naidu, V. G. M.; Srinivasulu, G.; Shankaraiah, N. *European Journal of Medicinal Chemistry* **2016,** *118*, 34.

27. Li Sun, N. T., Flora Tang, Harald App, Peter Hirth, Gerald McMahon, and Cho Tang*. *J. Med. Chem.* **1998,** *41*, 2588.

28. Henise, J. C.; Taunton, J. *Journal of Medicinal Chemistry* **2011,** *54*, 4133.

29. Kusakabe, K.; Ide, N.; Daigo, Y.; Tachibana, Y.; Itoh, T.; Yamamoto, T.; Hashizume, H.; Hato, Y.; Higashino, K.; Okano, Y.; Sato, Y.; Inoue, M.; Iguchi, M.; Kanazawa, T.; Ishioka, Y.; Dohi, K.; Kido, Y.; Sakamoto, S.; Yasuo, K.; Maeda, M.; Higaki, M.; Ueda, K.; Yoshizawa, H.; Baba, Y.; Shiota, T.; Murai, H.; Nakamura, Y. *Journal of Medicinal Chemistry* **2013,** *56*, 4343.

30. Liao, J. J. L. *Journal of Medicinal Chemistry* **2007,** *50*, 409.

31. McGregor, M. J. *Journal of Chemical Information and Modeling* **2007,** *47*, 2374.

32. Zhang, J.; Wang, J.; Guo, Q. Q.; Wang, Y.; Zhou, Y.; Peng, H. Z.; Cheng, M. S.; Zhao, D. M.; Li, F. *Cancer Letters* **2014,** *349*, 159.

33. Hopkins, A. L.; Groom, C. R.; Alex, A. *Drug Discovery Today* **2004,** *9*, 430.

34. Keseru, G. M.; Makara, G. M. *Nature Reviews Drug Discovery* **2009,** *8*, 203.

35. Leeson, P. D.; Springthorpe, B. *Nature Reviews Drug Discovery* **2007,** *6*, 881.

36. Lipinski, C. A.; Lombardo, F.; Dominy, B. W.; Feeney, P. J. *Advanced Drug Delivery Reviews* **2012,** *64*, 4.

37. Wager, T. T.; Hou, X. J.; Verhoest, P. R.; Villalobos, A. *Acs Chemical Neuroscience* **2010,** *1*, 435.

38. McMahon, G. T., Peng Cho; Sun, Li *US 6486185 B1 20021126*. **2002**.

39. Shenoy, N. S., Waranush,. *PCT Int. Appl. (2001), WO 2001037820 A2 20010531*. **2001**.

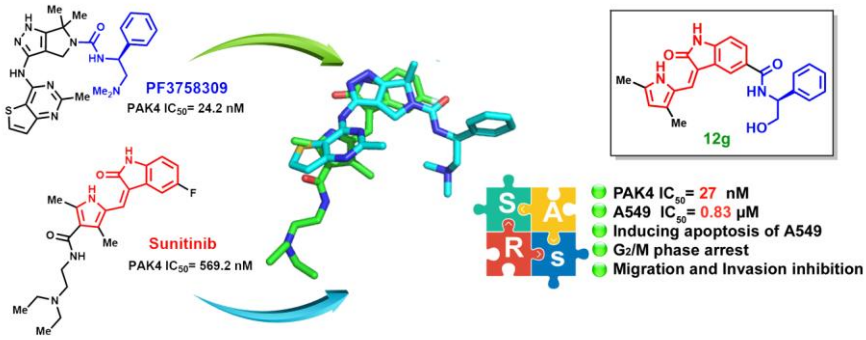

**Highlights**

- Twenty four indolin-2-one derivatives were synthesized.
- All the compounds were screened for *in vitro* PAK4 inhibition assay.
- Three of the compounds (**11b**, **12d**, **12g**) displayed promising enzymatic activity.
- Compound **12g** : Inducing apoptosis, G2/M phase arrest, Migration and Invasion inhibition by regulating PAK4-LIMK1-cofilin signalling pathway.
- Docking and ADME profiling of **12g** are reported.